THE ASTROPHYSICAL JOURNAL, 444:64–70, 1995 May 1

THE *HUBBLE SPACE TELESCOPE* QUASAR ABSORPTION LINE KEY PROJECT. V. REDSHIFT EVOLUTION OF LYMAN LIMIT ABSORPTION IN THE SPECTRA OF A LARGE SAMPLE OF QUASARS[1]

ERIK A. STENGLER-LARREA,[2,3] ALEC BOKSENBERG,[3] CHARLES C. STEIDEL,[4] W. L. W. SARGENT,[5]
JOHN N. BAHCALL,[6] JACQUELINE BERGERON,[7] GEORGE F. HARTIG,[8] BUELL T. JANNUZI,[6,9]
SOFIA KIRHAKOS,[6] BLAIR D. SAVAGE,[10] DONALD P. SCHNEIDER,[6,11]
DAVID A. TURNSHEK,[12] AND RAY J. WEYMANN[13]

Received 1993 December 2; accepted 1994 October 17

ABSTRACT

Using a sample of 119 QSOs, containing objects we have selected having previously available high quality ground-based and *IUE* spectral observations, together with *Hubble Space Telescope* (*HST*) observations of 26 QSOs from Bahcall et al. (1993, 1995) and Impey et al. (1995) and new optical observations of 41 objects by Steidel & Sargent (1995), we study the redshift evolution of Lyman limit absorption systems (LLSs; $\tau > 1.0$) over the redshift range $0.32 \leq z_{\rm LLS} \leq 4.11$. The *HST* observations significantly improve the determination of the low redshift ($0.4 \leq z_{\rm LLS} \leq 1.4$) distribution. We find the effect which may have been responsible for the apparent strong evolution at $z_{\rm LLS} \geq 2.5$ found by Lanzetta (1991), which led him to consider a broken, not single, power law as a better description of the redshift distribution of LLSs. After removing objects which may bias our sample, leaving a total of 169 QSOs, we find the distribution is well described by a single power law, and obtain for the number density as a function of redshift the form $N(z) = N_0(1+z)^\gamma$ with $\gamma = 1.50 \pm 0.39$ and $N_0 = 0.25^{-0.10}_{+0.17}$, consistent with a constant comoving density of absorbers in a Friedmann universe with $q_0 = 0$ but indicating evolution if $q_0 = \frac{1}{2}$.

Subject headings: quasars: absorption lines — ultraviolet: galaxies

1. INTRODUCTION

Narrow-line absorption systems that are optically thick to Lyman continuum radiation are found in the spectra of QSOs over a wide range in redshift. Typical strong lines of the Lyman-α forest indicate a neutral hydrogen column density N(H I) $\sim 10^{15}$ cm^{-2}, whereas N(H I) $\sim 10^{17}$ cm^{-2} is needed to produce an easily observable Lyman discontinuity. With optical depth $\tau \gtrsim 1$, a Lyman limit system (LLS) is so conspicuous that it can be readily identified even in spectra of low resolution and low signal-to-noise ratio. As Tytler (1982) first showed, with the use even of relatively low-quality *IUE* data combined with optical data, LLSs provide a useful diagnostic of the evolution of cosmologically distributed absorbers over an extensive range in redshift. LLSs with $\tau \gtrsim 1$ absorb most of the ultraviolet radiation blueward of the Lyman discontinuity and thus exert a considerable influence on the local level of the metagalactic flux of ionizing radiation due to QSOs and galaxies (e.g., Bechtold, Green, & York 1987; Bajtlik, Duncan, & Ostriker 1988). Thus the statistics and evolution of LLSs are particularly important because the metagalactic flux is thought to play a key role in ionizing the intergalactic medium and the Lyman-α clouds.

Following Tytler's pioneering work the redshift evolution of LLSs has been studied by Bechtold et al. (1984), Lanzetta (1988), Sargent, Steidel, & Boksenberg (1989, hereafter SSB) and Lanzetta (1991). With their substantial body of new data supplementing existing data SSB found no evolution in the properties of the absorbing objects over the range $0.67 \leq z_{\rm LLS} \leq 3.58$. Lanzetta (1991) also found no evolution, over the limited range $0.36 \leq z_{\rm LSS} \leq 2.5$; however, with additional observations from Lanzetta (1991), he obtained the striking result that beyond $z \sim 2.5$ there is a very strong increase with redshift in the rate of incidence of the LLSs. Lanzetta concluded that the contrasting strong decrease in the rate of incidence of C IV absorbers over a similar redshift range observed by Sargent, Boksenberg, & Steidel (1988) and by Steidel (1990) is most naturally interpreted as evolution of the ionization state of the absorbers and not due to progressive chemical enrichment as had been suggested by these workers. Some recent theoretical investigations have been based upon the presumed two power-law dependence of the number density of LLSs (e.g., Murakami & Ikeuchi 1993; Fan & Chen 1993). Here we add *HST* data from the *HST* Quasar Absorption Line Key Project (Bahcall et al. 1993, 1995) and from Impey et al. (1995), and new optical data from Steidel & Sargent (1995),

[1] Based on observations with the NASA/ESA *Hubble Space Telescope*, obtained at the Space Telescope Science Institute, which is operated by the Association of Universities for Research in Astronomy, Inc., under NASA contract NAS 5-26555.

[2] Institute of Astronomy, Madingley Road, Cambridge CB3 0HA, UK.
[3] Royal Greenwich Observatory, Madingley Road, Cambridge CB3 0EZ, UK.
[4] Physics Department, Massachusetts Institute of Technology, Room 6-201, Cambridge, MA 02139.
[5] Robinson Laboratory 105-24, California Institute of Technology, Pasadena, CA 91125.
[6] Institute for Advanced Study, School of Natural Sciences, Princeton, NJ 08540.
[7] Institut d'Astrophysique de Paris, CNRS, 98 bis Boulevard Arago, F-75014 Paris, France.
[8] Space Telescope Science Institute, 3700 San Martin Drive, Baltimore, MD 21218.
[9] Hubble Fellow.
[10] Department of Astronomy, University of Wisconsin, Madison, WI 53706.
[11] Department of Astronomy and Astrophysics, The Pennsylvania State University, University Park, PA 16802.
[12] Department of Physics and Astronomy, University of Pittsburgh, PA 15260.
[13] The Observatories of the Carnegie Institution of Washington, 813 Santa Barbara Street, Pasadena, CA 91101.

and exclude poor quality and severely biased spectral data following a re-examination of all available published material. We find no evidence for the onset of strong evolution of LLSs at high redshifts.

After a brief description of the statistical method in § 2 we present the data used and their treatment in this paper in § 3 and § 4. The analysis and results are given in § 5 and our conclusions are summarized in § 6.

2. STATISTICS OF THE LYMAN LIMIT SYSTEMS

In a standard Friedmann universe the number density of absorbers per unit redshift range $dN/dz \equiv N(z)$ is given by

$$N(z) = N_0(1 + z)(1 + 2q_0 z)^{-1/2}$$

(Bahcall & Peebles 1969; Sargent et al. 1980), where

$$N_0 = (c/H_0)\Phi_0 \pi R_0^2 ,$$

and assuming that the product of the comoving number density of absorbers (Φ_0) and their mean cross section (πR_0^2) does not evolve with redshift. Using the generally adopted representation of the observations as a power law of the form

$$N(z) = N_0(1 + z)^\gamma ,$$

evolution is indicated by $\gamma \neq 1$ for $q_0 = 0$ and $\gamma \neq 0.5$ for $q_0 = \frac{1}{2}$.

For LLS absorbers one must allow for the fact that a strong system at a given redshift prevents discovery of LLSs at lower redshifts. We follow Tytler (1982) who introduced the idea of using survival statistics encountered in biomathematics, obtaining the distribution of LLSs in redshift as a maximum likelihood (ML) estimate which does not assume any binning of the data (see SSB, but note that in their expression (9) the denominator should be taken to the square root). The different binnings shown in the figures throughout this paper are only for purpose of display and were not used in the generation of the ML estimations.

3. THE DATA SAMPLES

We assembled our initial database, which we call S1, as follows. We began with the 53 new observations presented in SSB and the nine in Bechtold et al. (1984). From Lanzetta (1991) we took the 43 new objects which were not observed by SSB. We then added the 25 objects in Tytler (1982) and the 54 objects contained in the compilation of Lanzetta (1988) which were not present in any of the previously mentioned samples. In total the sample gives us data from 184 objects. Redshifts below 2.5 are covered by the spectra of 35 of these objects.

Throughout this paper we adopt $\tau \geq 1$ as the condition for inclusion of LLSs into the statistical analysis, following most other workers. SSB in their analysis chose $\tau \geq 1.5$; we made the detections in their new sample complete to $\tau \geq 1$ by adding two of their systems for which we estimated $1.0 \leq \tau \leq 1.5$ from their published spectra: $z_{\rm LLS} = 2.856$ in Q0055−264 and $z_{\rm LLS} = 2.635$ in Q0112+0.29.[14]

Because of the various source material this sample lacks consistency in the quality selection criteria. We therefore decided to reexamine the available spectra and be more selective, in an attempt to homogenize the quality of our database, and included only those objects having appropriate wavelength coverage which we estimated to be of a quality good enough for the reliable detection of LLSs with $\tau \geq 1$. For the *IUE* data we used the spectral compilation in the *IUE* Uniform Low-Dispersion Archive (Courvoisier & Paltani 1992) and for the rest we examined the spectra published in the original papers referred to in the authors' listings. Table 1 lists the objects we selected from S1 for this revised sample, a total of 119. To these we added 26 *HST* objects covering the low-redshift region (Bahcall et al. 1993, 1995; Impey et al. 1995). We note that in Bahcall et al. (1993) five LLSs with $\tau \geq 1$ are listed. We now recognize two more LLSs with $\tau > 1$, which had been determined to have $\tau < 1$ using the unconventional definition described in Schneider et al. 1993; we include these in Table 1. We have excluded five objects listed in their LLS sample: 1130−106Y, because of its low signal-to-noise ratio; PKS 1206+459 and MC 1215+113, for the non-uniformity of their continua, which could have obscured LLSs; PG 1407+265 and PKS 1656+053, because their redshifts are uncertain since neither the Lyman-α not the Lyman-β/O VI emission bumps are present at the expected positions. Finally, we added an additional sample of 41 objects with new optical observations from Steidel & Sargent (1995), of which 14 replacing those listed by Lanzetta (1988, 1991) are marked with the superscript "m" in Table 1. The total of 186 objects makes up our revised and extended database, which we call S2.

4. REDSHIFT DETERMINATIONS

Because of the blending of the higher absorption lines of the Lyman series the effective Lyman limit is shifted longward (Smith et al. 1981).

In the various previous statistical analyses different techniques were used to take this into account when determining the redshift at which a LLS was found. Tytler (1982) used the better determined redshifts from the metal line systems associated with some of the LLSs to establish the systematic difference between these redshifts and those corresponding to the wavelength at which the flux reaches half the intensity it had longward of the apparent onset of the Lyman limit absorption. He found that $z_{\rm LLS}$ is closely determined when the wavelength at the half-intensity flux is divided, for his sample, by 918 instead of 912 Å. Lanzetta (1988) adopted the redshifts of associated metal lines if such were known. If not, he applied Tytler's (1982) technique unless $\lambda_{\rm LLS}$ (variously determined) was given in the original publication. He used a similar procedure in Lanzetta (1991). SSB chose to define $\lambda_{\rm LLS}$ by determining the point at which the flux reaches its minimum, not applying any correction to obtain $z_{\rm LLS}$. Steidel & Sargent (1995) followed the same procedure. Bahcall et al. (1993) obtained their $z_{\rm LLS}$ values by dividing the wavelength at half intensity by 912 Å.

Although this variety of methods does not lead to significant inaccuracies in our context, for consistency we reassessed all the spectra available. We divided the wavelength at what we judged to be the minimum intensity by 914 Å, which we determined for the combined sample from an examination of all cases for which metal systems were known and listed in SSB, York et al. (1991) and Steidel & Sargent (1995).

With regard to the minimum wavelengths at which LLSs could be observed, most authors systematically excluded a small range at the short wavelength end of their spectra to avoid confusion with possible strong absorption lines terminated at the spectrum limit. In our re-examination of the spectra we adopted the following method: in cases where a drop of the

[14] Later (in our sample S2) we excluded this object, among others, on quality grounds.

TABLE 1

QUASARS AND LYMAN LIMIT ABSORPTION SYSTEMS ($\tau \geq 1$) IN SAMPLE S2

QSO	z_{em}	λ_{min} (Å)	λ_{LLS}[a] (Å)
IUE (Courvoisier & Paltani 1992)			
0002+051	1.890	1720	...
0003+157	0.450	1250	...
0232−042	1.434	1250	...
0237−233	2.224	2450	...
0405−123	0.574	1250	...
0414−060	0.773	1250	...
0454−220	0.534	1250	1350
0637−752	0.654	1250	...
0742+318	0.462	1250	...
0935+417	1.937	1970	2250
0955+326	0.533	1250	...
0957+561A	1.390	1250	2170[b]
0958+551[c]	1.754	1970	2495[b]
1007+417	0.613	1250	...
1101−264	2.148	1970	2588
1103−006	0.426	1250	...
1115+080	1.722	1250	...
1137+660	0.652	1250	...
1148+549	0.969	1250	...
1156+295	0.729	1250	...
1225+317	2.219	1250	2580
1247+268	2.041	1250	2125
1248+401	1.03	1250	1585
1318+290B	0.549	1250	...
1421+330[d]	1.904	2400	...
1522+101	1.321	1250	...
1526+285	0.450	1250	...
1630+3744	1.466	1250	...
1641+399	0.594	1250	...
1718+481	1.084	1250	...
2128−123	0.501	1250	1305
2302+029	1.044	1250	...
2308+098	0.432	1250	...
Bahcall et al. (1993, 1995)			
0024+223	1.118	1250	...
0044+030	0.624	1280	...
0122−002	1.070	1630	...
0349−144[e]	0.614	1250	...
0850+440[f]	0.513	1250	...
0916+512[g]	0.553	1250	...
1022+193[h]	0.828	1250	1390
1038+063[i]	1.270	1250	1310
1040+122[j]	1.028	1250	...
1055+201	1.110	1250	1864
1136−133	0.554	1250	...
1244+32B	0.949	1250	...
1252+112	0.870	1250	...
1259+593	0.472	1180	...
1317+274[k]	1.022	1250	1513
1333+176	0.554	1250	...
1338+416	1.219	1250	...
1340+286	0.905	1250	...
1347+536[l]	0.976	1330	...
1352+011	1.121	1250	1518
1354+193	0.720	1250	1325
1415+172	0.821	1250	...
1424−115	0.805	1250	1482
1618+174	0.555	1250	...
2251+155	0.859	1400	...
Impey et al. (1995)			
1634+706	1.334	1580	1817
Tytler (1982)			
0002−422	2.76	3300	...
0049−393	2.85	3200	3439
0130−403	3.02	3200	3470
0138−381	2.87	3350	...
0140−306	3.13	3200	3658
0207−398	2.81	3200	...
0537−286	3.11	3300	3630
1402+044	3.20	3500	3878[b]
2204−408	3.17	3400	...
Lanzetta (1988)			
0855+182	2.619	3200	...
1127+078	2.661	3260	...
1136+122	2.894	3450	...
1352+108	3.150	3600	...
1510+105	3.053	3500	...
SSB			
0000−263	4.111	3250	4024
0001+087	3.243	3250	3654
0004+171	3.289	3200	3539
0014+813	3.384	3250	3477
0029+073	3.259	3200	3702
0045−036	3.135	3200	3493
0054−284	3.616	3500	4182[b]
0055−264	3.656	3250	3524
0101−304	3.150	3200	3562
0102−190	3.035	3300	3593
0114−089	3.160	3400	...
0132−198	3.130	3250	...
0143−015	3.138	3200	...
0148−097	2.848	3350	...
1153+045	2.991	3200	...
0207−003	2.856	3300	...
0216+080	2.993	3250	...
0249−184	3.205	3200	3342
0249−222	3.202	3250	3591
0256−000	3.374	3250	3730
0301−006	3.223	3250	3600
0302−003	3.286	3150	3219
0308+190	2.835	3200	...
0308−193	2.752	3200	...
0316−203	2.865	3300	...
0334−204	3.130	3700	...
0352−275	2.819	3200	...
0420+007	2.918	3250	...
0449−134	3.093	3300	3614
0528−250	2.779	3250	3501[b]
0636+680	3.174	3200	3565
0624+449	3.406	3200	3884
0731+653	3.033	3200	3568
0805+046	2.873	3400	3330
0830+115	2.976	3450	...
0941+261	2.906	3250	...
0956+122	3.301	3300	3736
1017+109	3.156	3300	3692
1836+511	2.827	3200	3521[b]
2000−330	3.777	3250	4148
2038−012	2.783	3250	3395[b]
2048+312	3.185	3400	...
2126−158	3.261	3250	3623
2233+131	3.295	3200	3798
2233+136	3.209	3200	3735
2311−036	3.041	3300	...
2348−011	3.005	3200	3593[b]
2359+003	2.896	3250	...
2359−022	2.817	3350	...
2359+068	3.234	3200	...
Lanzetta (1991)			
0001+0842	3.257	3200	3665
0041−2638	3.070	3400	...

TABLE 1—*Continued*

QSO	z_{em}	λ_{min} (Å)	λ_{LLS}[a] (Å)	QSO	z_{em}	λ_{min} (Å)	λ_{LLS}[a] (Å)
0042−269........	3.358	3400	3903	1208+1011	3.803	3200	3364
0042−2627	3.296	3200	3785	1209+1524	3.049	3200	3725[b]
0047−233........	3.422	3500	3970	1223+1753	2.939	3200	3594[b]
0058−292........	3.093	3200	3380	1244+1129	3.138	3200	3753[b]
0112−303........	2.985	3200	3470	1251+3643	2.976	3200	3303
0112−273........	2.894	3200	3310	1305+2941	3.018	3200	3628[b]
0115−303........	3.249	3350	...	1317−0507	3.712	3200	3529
0136+1737	2.716	3200	...	1330+0108	3.532	3200	4034
0336−0142	3.197	3500	3765	1337+113........	2.916	3200	3467[m]
0347−3819	3.228	3300	3690	1340+0959	2.932	3200	3393
0351−3904	3.010	3250	...	1358+3908	3.271	3200	3904[b,m]
0420−3851	3.123	3200	3740[b]	1400+0935	2.973	3200	3398
0938+1159	3.191	3650	...	1400+1126	3.164	3345	...[m]
1052+043........	3.391	3200	3715	1410+0936	3.317	3200	3778[m]
1124+5706	2.890	3400	...	1442+101........	3.555	3200	...
1159+010........	3.269	3550	3600	1451+1223	3.247	3200	3812[b,m]
1205−303........	3.036	3400	3690[b]	1455+1221	3.042	3200	3337[m]
1209+0919	3.297	3400	3800	1511+091........	2.874	3200	...
1937−1009	3.787	3600	4175	1548+0917	2.747	3200	3370
2239−384........	3.554	3700	4110[b]	1607+1819	3.106	3200	3425[m]
				1614+0506	3.209	3200	3624
Steidel & Sargent (1995)				1631+3722	2.932	3400	...[m]
				2125−1335	2.914	3446	...
0056+0126	3.147	3200	3602	2132+0126	3.191	3200	3553
0428−1342	3.245	3245	...[m]	2211+0119	3.096	3200	3501
0905+1507	3.166	3200	...	2231−0015	3.016	3200	3339[m]
0932+3646	2.851	3145	...[m]	2244−2218	2.849	3200	...
1003−0236	2.865	3145	...	2336+1036	2.847	3200	3415
1033+1342	3.087	3145	...[m]	2342+1229	2.746	3200	...
1142+1015	3.148	3200	3626	2342+0852	2.781	3200	3312
1159+1223	3.510	3200	4144[b]	2344+1225	2.763	3200	3414
1206+1155	3.108	3200	3680[m]	2351+0840	2.738	3200	3335[b]

[a] This is the observed wavelength at the minimum flux as judged in this paper. We divided these values by 914 Å to obtain z_{LLS} (see text).

[b] Objects excluded from the statistical analysis because they have a LLS within 5000 km s^{-1} of the QSO redshift.

[c] Mkn 132.

[d] Mkn 679.

[e] 3C 95.

[f] US 1867.

[g] NGC 2841 UB3.

[h] 4C 19.34.

[i] 4C 06.41.

[j] 3C 245.0.

[k] TON 153.

[l] 4C 53.28.

[m] Objects from Steidel & Sargent 1995 which in our table have replaced earlier observations listed by Lanzetta 1988, 1991.

flux was seen close to the end of the spectrum it was not accepted as a LLS, and the region was excluded, unless the spectrum extended on sufficiently to distinguish the possible LLS from a deep absorption line (we rejected, for example, the possible system in Q0132−198 evident in the spectrum shown in SSB); otherwise, the minimum recorded wavelength or the limit at which the signal-to-noise ratio per pixel reduced to 2 was taken as the end-point of the spectrum. Since a reduction in signal-to-noise ratio is also expected from absorption by a LLS, extreme care was taken and the estimate was made redward of the candidate LLS if such were present.

5. ANALYSIS AND RESULTS

It has been observed in some QSO samples that there is a preferential tendency for absorption to occur close to the emission redshift of a QSO. Moreover, the QSO itself may introduce related self-absorption or strongly influence the ionization state of galaxies in its immediate vicinity. Accordingly, in our analyses we have employed only redshifts for which the velocity relative to the QSO ≥ 5000 km s^{-1}. This reduces our initial sample, S1, to 154 objects and our sample S2 to 169 objects.

We operated first on S1. We obtain for the ML value of the power law index $\gamma = 0.95 \pm 0.50$, and $N_0 = 0.60^{-0.28}_{+0.50}$. We show in Figure 1 how such a power law relates to the number density $N(z)$ in different redshift bins, calculated directly from the data and independently of the estimation of γ. The normalization of the curve was done by forcing the area below it to equal the total area contained in the different bins. We found that the appearance of the fit is very sensitive to the specific binning of the data: if we use bins similar to those of Lanzetta (1991) the same data seem to fit poorly to the ML estimated curve and indeed suggest a broken power law distribution (Fig. 2) as claimed by him.

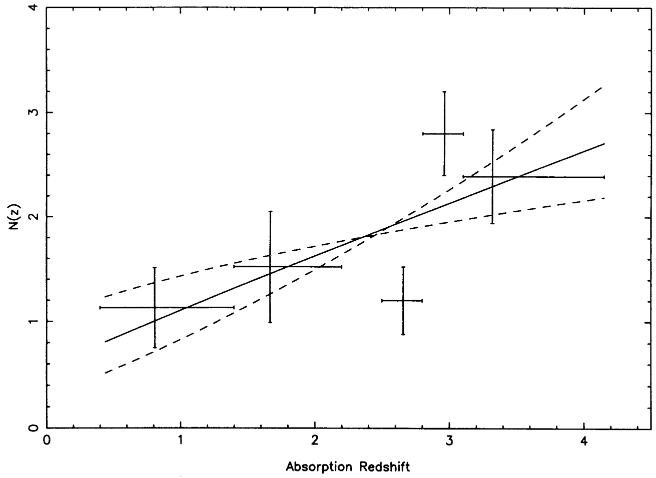

FIG. 1.—Redshift evolution of the LLSs from our sample S1, using 154 objects in total. In this and all other figures we exclude objects having a LLS with apparent "ejection" velocity ≤ 5000 km s^{-1}. The full line represents the maximum likelihood power law fit to the data, normalized as described in the text, with $\gamma = 0.95$ and $N_0 = 0.60$. The dashed lines represent the 1 σ errors on these estimates.

The unrevised *IUE* data in S1, as were used by SSB and Lanzetta (1991), give at the redshifts covered by the *HST* sample ($0.4 \leq z_{\rm LLS} \leq 1.4$) $\langle N(z) \rangle = 1.13 \pm 0.38$ (Fig. 1), somewhat higher than the value obtained by combining our revised *IUE* data and the *HST* data in S2, $\langle N(z) \rangle = 0.70 \pm 0.20$. The *HST* data alone give $\langle N(z) \rangle = 0.94 \pm 0.33$ and the revised *IUE* sample gives $\langle N(z) \rangle = 0.47 \pm 0.23$. Table 2 summarizes the values obtained at low redshifts for the different samples. The influence of the higher number density at low redshifts obtained with the *IUE* sample in S1 has the effect of flattening the overall evolutionary behavior giving, as we have found, $\gamma \sim 1$ for a single power law. We note that this is contributory to Lanzetta's (1991) claim that a broken power law is a better description of the evolutionary behavior.

We observe that in Figures 1 and 2 the region near $z_{\rm LLS} = 2.5$ appears significantly depleted in number of LLSs. The apparent underdensity occurs at the inevitably poor-quality

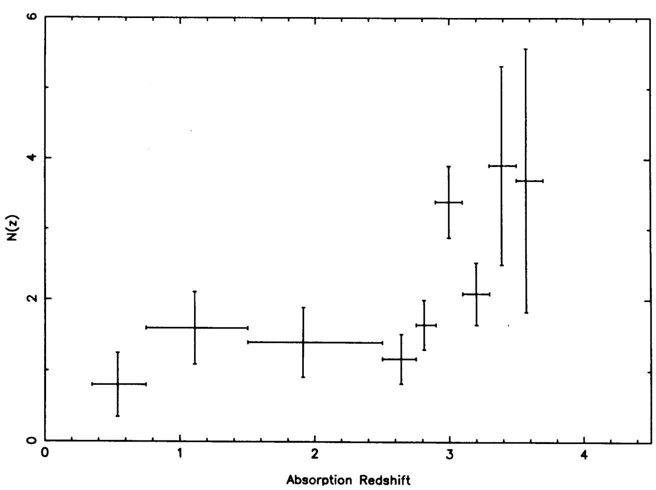

FIG. 2.—Redshift evolution of the LLSs from our sample S1 but with binning similar to Lanzetta (1991). The same power law fit as in Fig. 1 applies here.

TABLE 2

VALUES OF $N(z)$ AT REDSHIFTS $0.4 \leq z \leq 1.4$

Sample	$\langle N(z) \rangle$	$\langle z_{\rm LLS} \rangle$
IUE (S1)	1.13 ± 0.38	0.81
IUE (S2)	0.47 ± 0.23	0.78
HST (S2)	0.94 ± 0.33	0.62
IUE + *HST* (S2)......	0.70 ± 0.20	0.69

short-wavelength end of the optical spectra ($z_{\rm LLS} = 2.5$ at 3200 Å). Figure 3*a* shows that a significant fraction of the optical spectra taken from the literature covers this problematic region. We checked whether this depletion effect is also present in the SSB sample, since it did not seem to be indicated by their data (their Fig. 4). A deficit indeed becomes apparent with an appropriate binning, which we show in Figure 4: here we use their full data set, imposing $\tau \geq 1$, and, excluding from the ML estimation the region $2.5 \leq z_{\rm LLS} \leq 2.7$, we obtain $\gamma = 1.14 \pm 0.61$[15] and $N_0 = 0.44^{-0.24}_{+0.48}$. We assert that Lanzetta (1991) underestimated the significance of this observational limitation near the atmospheric cutoff and was led to believe the presence of a real break in the redshift evolution at $z_{\rm LLS} \sim 2.5$.

We paid special attention to the region near $z_{\rm LLS} = 2.5$ when compiling the revised sample S2. Figure 3*b* shows that after our removal of poor quality regions from the available spectra a smaller fraction remain with an acceptable quality in the range near the atmospheric cutoff. With our revisions the apparent deficit loses its significance, and we obtain a single power law with $\gamma = 1.50 \pm 0.39$ and $N_0 = 0.25^{-0.10}_{+0.17}$ as our best estimates from our residual S2 database of 169 objects. In Figure 5 we show the redshift distribution for these data, illustrated with bins displayed as in Figure 1.

6. SUMMARY AND CONCLUSIONS

We have compiled a large sample of QSOs with redshifts in the range $0.32 \leq z_{\rm LLS} \leq 4.11$ containing objects with previously available optical and ultraviolet spectral observations useful for LLS studies. We include *HST* observations (Bahcall et al. 1993, 1995) and new optical observations (Steidel & Sargent 1995). In the process of considering candidates for our list we were stringent in assessing the quality of the spectral data and included data from only those objects and their specific spectral regions which we judged to be of sufficient quality for the reliable detection of LLSs with $\tau \geq 1$. Our full database (S2) contains 186 objects in total. After excluding all objects having a LLS with apparent ejection velocity ≤ 5000 km s^{-1} there remain 169 objects, with a total of 80 LLSs. Our main conclusions from a study of this sample are as follows:

1. A study of the redshift evolution of LLSs is most reliable when it is independent of the binning of the data, since the appearance of the distribution is very sensitive to the choice of bins.

2. Our evaluation of the number density at low redshifts ($0.40 \leq z_{\rm LLS} \leq 1.40$), now including the recently published *HST*-observed objects (Bahcall et al. 1993, 1995; Impey et al 1995), gives a value, $\langle N(z) \rangle = 0.70 \pm 0.20$, which is lower

[15] The value $\gamma = 0.68 \pm 0.54$ quoted in SSB was influenced by the inclusion, in their full sample, of systems incorrectly taken from the literature with $\tau \geq 1$, while they applied $\tau \geq 1.5$ for their new observations, thus making their sample inhomogeneous (Steidel 1993).

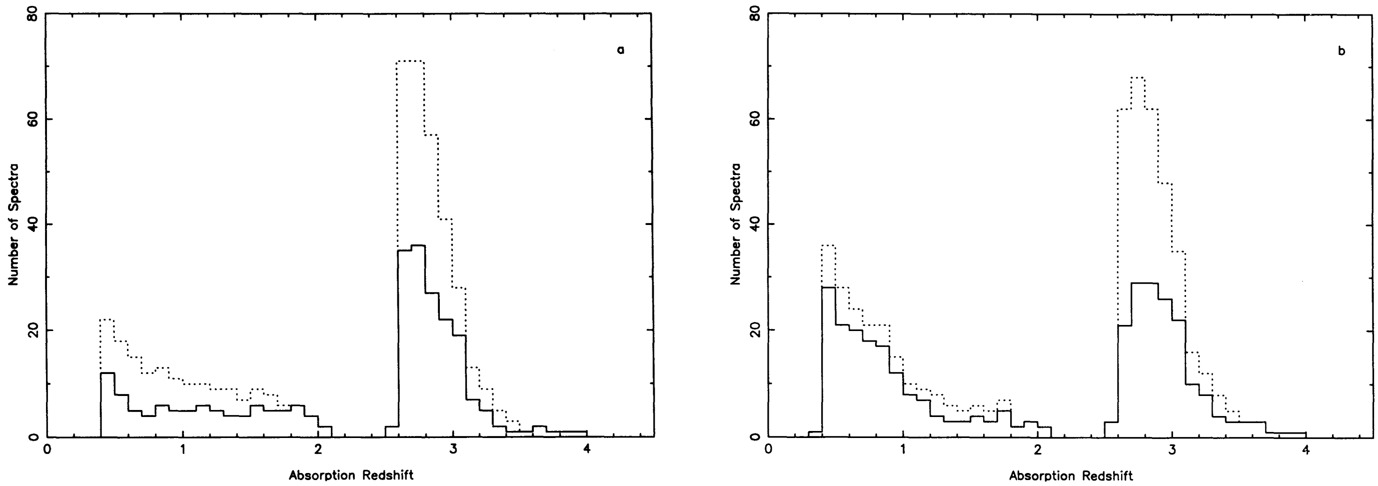

FIG. 3.—Number of spectra covering different redshift bins: (*a*) in sample S1; (*b*) in sample S2. The full line indicates the aggregated spectral coverage where no LLSs were detected; the broken line indicates the additional coverage shortward of detected LLSs with $\tau \geq 1$.

than—but not statistically different from—the value obtained from the sample of *IUE*-observed objects used by SSB and Lanzetta (1991), $\langle N(z) \rangle = 1.13 \pm 0.38$.

3. The inclusion of the poor spectral quality region $2.5 \leq z_{\rm LLS} \leq 2.7$ without special care has led to the apparent underdensity near $z_{\rm LLS} = 2.5$ shown in Lanzetta (1991). Our reassessment of the data has reduced the effect to insignificance. The effect explains Lanzetta's conclusion that a broken, not single, power law is a better description of the redshift distribution of LLSs. Using our higher quality and more extended sample we do not find Lanzetta's (1991) distribution and find no cause to depart from the form $N(z) = N_0(1 + z)^{\gamma}$.

4. From our residual S2 list, containing 169 objects with a total of 80 LLSs, we obtain for the redshift distribution of LLSs over our whole redshift range the values $\gamma = 1.50 \pm 0.39$ and $N_0 = 0.25^{-0.10}_{+0.17}$. This is consistent within the errors with a constant comoving density of absorbers in a Friedmann universe with $q_0 = 0$, but indicates significant evolution if $q_0 = \frac{1}{2}$. The properties we have derived for the LLS absorbers are not significantly different from those found by Steidel & Sargent (1992) for a population of Mg II absorbers, over the common redshift interval extending to $z \sim 2$.

We thank Richard Hunstead, Max Pettini, and especially Charles Jenkins for assistance in the statistical analysis, Lisa Storrie-Lombardi, Patrick Petitjean, Filippo Zerbi, and Alberto Fernández Soto for useful comments, and Jim Lewis and Keith Lipman for assistance with software and manuscript, respectively. This work was partially supported by NASA contract NAG 5-1618 and grants GO-2424.01 and HF-1045.01-93A from the Space Telescope Science Institute, which is operated by the Association of Universities for Research in Astronomy Inc., under NASA contract NAS 5-26555.

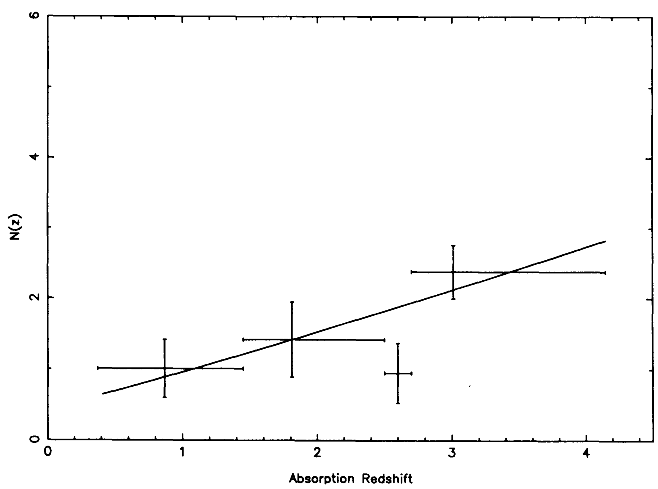

FIG. 4.—Redshift evolution of the LLSs in SSB's sample, with a binning which shows clearly that a deficit at $2.5 \leq z_{\rm LLS} \leq 2.7$ occurs also in this data set. The fitted evolutionary behavior has been estimated excluding the data in the range $2.5 \leq z_{\rm LLS} \leq 2.7$ and corresponds to $\gamma = 1.14 \pm 0.61$ and $N_0 = 0.44^{-0.24}_{+0.48}$.

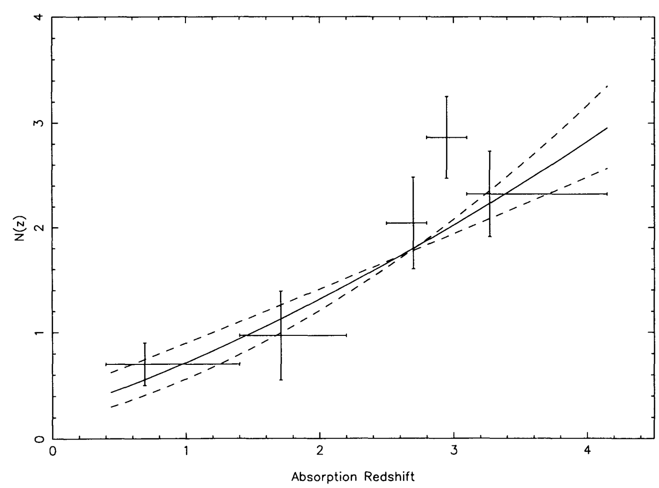

FIG. 5.—Redshift evolution of LLSs as estimated from our sample S2, using 169 objects in total. The full line represents the distribution $N(z) = 0.25(1 + z)^{1.50}$; the dashed lines represent the 1 σ errors on these estimates.

REFERENCES

Bahcall, J. N., et al. 1993, ApJS, 87, 1
———. 1995, ApJS, submitted
Bahcall, J. N., & Peebles, P. J. E. 1969, ApJ, 156, L7
Bajtlik, S., Duncan, R. C., & Ostriker, J. P. 1988, ApJ, 327, 570
Bechtold, J., Green, R. F., Weymann, R. J., Schmidt, M., Estabrook, F. B., Sherman, R. D., Wahlquist, H. D., & Heckman, T. M. 1984, ApJ, 281, 76
Bechtold, J., Green, R. F., & York, D. G. 1987, ApJ, 312, 50
Courvoisier, T. J.-L., & Paltani, S., eds. 1992, IUE-ULDA Access Guide No. 4A (ESA SP 1153)
Fan, X.-H., & Chen, J.-S. 1993, A&A, 277, L5
Impey, C. D., Petry, C. E., Malkan, M. A., & Webb, W. 1995, ApJ, in press
Lanzetta, K. M. 1988, ApJ, 332, 96
———. 1991, ApJ, 375, 1
Murakami, I., & Ikeuchi, S. 1993, ApJ, 409, 42
Sargent, W. L. W., Boksenberg, A., & Steidel, C. C. 1988, ApJS, 68, 535
Sargent, W. L. W., Steidel, C. C., & Boksenberg, A. 1988, ApJ, 334, 22
———. 1989, ApJS, 69, 703 (SSB)
Sargent, W. L. W., Young, P. J., Boksenberg, A., & Tytler, D. 1980, ApJS, 42, 41
Schneider, D. P., et al. 1993, ApJS, 87, 45
Smith, M. G., et al. 1981, MNRAS, 195, 437
Steidel, C. C. 1990, ApJS, 74, 37
———. 1992, PASP, 104, 843
———. 1993, private communication
Steidel, C. C., & Sargent, W. L. W. 1992, ApJS, 80, 1
———. 1995, in preparation
Steidel, C. C., Sargent, W. L. W., & Boksenberg, A. 1988, ApJ, 333, L5
Tytler, D. 1982, Nature, 298, 427
York, D. C., Yanny, B., Crotts, A., Carilli, C., Garrison, E., & Matheson, L. 1991, MNRAS, 250, 24